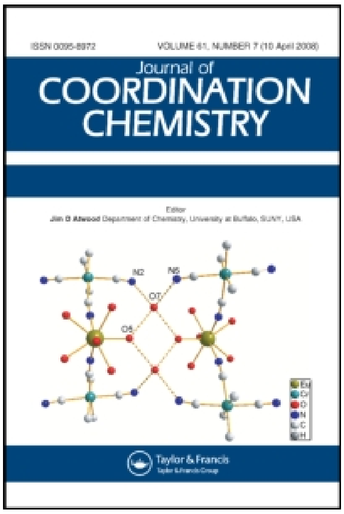

Journal of Coordination Chemistry

Publication details, including instructions for authors and subscription information:
http://www.informaworld.com/smpp/title~content=t713455674

Polymeric nickel(II) squarate complexes with imidazole derivatives: syntheses, crystal structures, spectroscopic and voltammetric studies

İbrahim Uçar[a]
[a] Faculty of Arts and Sciences, Department of Physics, Ondokuz Mayıs University, Kurupelit, Samsun, Turkey

To cite this Article Uçar, İbrahim(2008) 'Polymeric nickel(II) squarate complexes with imidazole derivatives: syntheses, crystal structures, spectroscopic and voltammetric studies', Journal of Coordination Chemistry, 61: 16, 2590 — 2600
To link to this Article: DOI: 10.1080/00958970801950011
URL: http://dx.doi.org/10.1080/00958970801950011

Journal of Coordination Chemistry
Vol. 61, No. 16, 20 August 2008, 2590–2600

Polymeric nickel(II) squarate complexes with imidazole derivatives: syntheses, crystal structures, spectroscopic and voltammetric studies

İBRAHIM UÇAR*

Faculty of Arts and Sciences, Department of Physics, Ondokuz Mayıs University,
Kurupelit, Samsun, 55139, Turkey

(*Received 6 June 2007; in final form 6 November 2007*)

Two squarate complexes of nickel(II), $[Ni(C_4O_4)(4\text{-Meim})_2(H_2O)_2]_n$ (**1**) (4-Meim: 4-methylimidazole) and $[Ni(C_4O_4)(his)_2]_n \cdot nH_2O$ (**2**) (his: histamine or 2-(4-imidazolyl)ethylamine), have been synthesized and characterized by X-ray diffraction, IR and UV–Vis techniques. The electrochemical properties of the nickel(II) complexes are investigated by cyclic voltammetry. In both complexes the Ni(II) ions have distorted octahedral geometry. Both structures comprise infinite chains parallel to [010] for **1**, $[10\bar{1}]$ for **2** built up of bis(monodentate) squarate-O^1,O^3 (μ-1,3) $C_4O_4^{2-}$ anions bridging $[Ni(4\text{-Meim})_2(H_2O)_2]$ (**1**) and $[Ni(his)_2]$ (**2**) units. These chains are held together by hydrogen bonds between the noncoordinated oxygens of the squarate anions and the water molecules, forming a two-dimensional sheet of Ni(II) ions. These sheets are held together by hydrogen bonds between the imidazole (**1**) or amine (**2**) hydrogens and noncoordinated squarate oxygens (**1** and **2**), or water (**2**) molecules. IR and UV–Vis spectra of both compounds agree with the observed crystal structure. The voltammetric behaviors of **1** and **2** were investigated in DMSO (dimethylsulfoxide) solution by cyclic voltammetry using $n\text{-Bu}_4NClO_4$ supporting electrolyte. Both complexes exhibit only ligand ($C_4O_4^{2-}$) centred electroactivity in the potential −0.2–1.4 V *versus* Ag/AgCl reference electrode. The squarate anion is oxidized in two consecutive steps to the corresponding radical monoanion and neutral form.

Keywords: Polymeric Ni(II) squarate complexes; X-ray crystal structure; IR; UV–Vis; Cyclic voltammetry

1. Introduction

Squaric acid, 3,4-dihydroxy-3-cyclobutene-1,2-dione ($C_4H_2O_4$), is a strong dibasic acid and has been studied for potential application to organic solar cells and optical recording devices [1, 2]. Because of the presence of several potential donor oxygen atoms, increasing attention has been devoted to the coordination chemistry of the squarate ligand, $C_4O_4^{2-}$, by both inorganic and bioinorganic chemists [3–5]. Squarate acts as a bridge between two or more metal atoms in mono- or polydentate coordination modes with first row transition metal ions [6, 7]. It coordinates to Fe(II), Fe(III), Ni(II) and Cu(II) complexes in a μ-1,3 fashion, giving binuclear [8–11]

---

*Email: iucar@omu.edu.tr

Journal of Coordination Chemistry
ISSN 0095-8972 print/ISSN 1029-0389 online © 2008 Taylor & Francis
DOI: 10.1080/00958970801950011

and chain structures [12, 13], whereas the μ-1,2 coordination mode has been reported for binuclear and chain complexes of Cu(II) and Pd(II) [14, 15]. The squarate anion, with Cu(II) and Ni(II), is a tetradentate ligand forming polynuclear compounds [16]. The chelating and bis-chelating coordination modes are only possible in complexes with larger metal ions, such as alkaline and rare-earth cations [17–19]. In our ongoing research on squaric acid, we have synthesized some mixed-ligand metal(II) complexes of squaric acid, and their structures have been reported [20–23]. In these compounds, squaric acid is a monodentate ligand [24, 25] or both a monodentate and a bidentate ligand [26], while in **1** and **2**, reported in the present study, it has μ-1,3 *bis*(monodentate) coordination between the Ni(II) ions. We have used histamine, an imidazole derivative, as ligand. Imidazole with two nitrogen atoms provides a potential binding site for metal ions in many biological systems [27]. Histamine effects many physiological and pathological processes, e.g. the regulation of micro-circulation and blood pressure, the stimulation of gastric secretion, the mediation of symptoms of allergy and inflammation, etc.; use in pharmacology makes it an attractive field for biochemical researchers [28]. Therefore, the present complexes of imidazole derivatives may be of interest in pharmacological studies.

2. Experimental

2.1. *General method*

All chemical reagents were analytical grade commercial products. Solvents were purified by conventional methods. The IR spectra were recorded on a Jasco 430 FT/IR spectrometer using KBr pellets and operating in the 4000–400 cm^{-1} range. UV–Vis spectra were obtained for aqueous solutions of the complexes (10^{-3} M) with a Unicam UV2 spectrometer in the range 900–190 nm. An EcoChemie Autolab-30 potentiostat with the electrochemical software package GPES 4.9 (Utrecht, Netherlands) was used for voltammetric measurements. A three electrode system was used: a Pt counter electrode, an Ag/AgCl reference electrode and a Pt wire electrode as working electrode. The potentiostat/galvonastat have an IR-compensation option. Therefore, the resistance due to the electrode surface was compensated throughout the measurements. Oxygen-free nitrogen was bubbled through the solution before each experiment. All experiments were carried out at room temperature.

2.2. *Syntheses of catena-poly[[diaquabis(4-methylimidazole-κN)nickel(II)]-μ_2-squarato-κO^1:O^3] (1) and catena-poly[[[bis(histamine-κ^{2}N:N′) nickel(II)]-μ_2-squarato-κO^1:O^3]monohydrate] (2)*

Squaric acid (0.57 g, 5 mmol) dissolved in 25 mL water, neutralized with NaOH (0.40 g, 10 mmol), was added to a hot solution of $NiCl_2 \cdot 2H_2O$ (0.81 g, 5 mmol) dissolved in 100 mL water. After stirring for 30 min, precipitates were filtered and washed with acetone to yield $Ni(C_4O_4) \cdot 2H_2O$. An aqueous solution of 4-methylimidazole (**1**) or histamine (**2**) (2 mmol, 20 mL) was added into aqueous solutions of these compounds (1 mmol, 20 mL), under stirring, and the mixtures were allowed to stand at room temperature. A few days later, well formed crystals were selected for X-ray studies.

2.3. *X-ray crystallography*

A suitable single crystal was mounted on a glass fibre and data collection was performed on a STOE IPDSII image plate detector using Mo-Kα radiation ($\lambda = 0.71019$ Å). Details of crystal structures are given in table 1. Data collection: Stoe X-AREA [29]. Cell refinement: Stoe X-AREA [29]. Data reduction: Stoe X-RED [29]. The structure was solved by direct methods using SHELXS-97 [30] and anisotropic displacement parameters were applied to non-hydrogen atoms in a full-matrix least-squares refinement based on F^2 using SHELXL-97 [30]. All aromatic and methyl hydrogens were positioned geometrically and refined by a riding model with U_{iso} 1.2 and 1.5 times, respectively, that of attached atoms; remaining H atoms were found by Fourier difference map. Molecular drawings were obtained using ORTEP-III [31].

3. Results and discussion

3.1. *Crystal structures of 1 and 2*

The crystal structures of both compounds consist of chains built up by squarato-O^1,O^3-bridged (μ-1,3) Ni(II) ions. Contrary to [Ni(C_4O_4)(H_2O)$_2$] [32], where all squarato oxygens are coordinated directly to Ni(II), forming a sheet structure, the

Table 1. The details of the crystal data and structure refinement for **1** and **2**.

Formula	$C_{12}H_{16}N_4O_6Ni$	$C_{14}H_{20}N_6O_5Ni$
Formula weight	370.98	411.05
Temperature (K)	297(2)	297(2)
Wavelength (Mo-Kα) (Å)	0.71073	0.71073
Crystal system	Monoclinic	Monoclinic
Space group	$P2_1/c$	$C2/c$
Unit cell dimensions (Å, °)		
a	8.668(7)	8.948(6)
b	7.935(6)	19.259(2)
c	11.130(1)	9.955(7)
β	103.914(6)	98.396(6)
Volume (Å^3)	743.1(8)	1697.3(2)
Z	2	4
Calculated density (g cm^{-3})	1.660(2)	1.608(2)
μ (mm^{-1})	1.343	1.184
F (000)	384	856
Crystal size (mm^3)	$0.24 \times 0.32 \times 0.41$	$0.22 \times 0.30 \times 0.40$
θ range (°)	1.88–27.06	2.11–27.93
Index ranges	$-11 \leq h \leq 8$ $-10 \leq k \leq 10$ $-14 \leq l \leq 14$	$-11 \leq h \leq 11$ $-25 \leq k \leq 25$ $-13 \leq l \leq 12$
Reflections collected	4580	11574
Independent reflections	1601 [$R_{(\text{int})} = 0.048$]	2010 [$R_{(\text{int})} = 0.058$]
Reflections observed (>2σ)	1370	1806
Absorption correction	Integration	Integration
Refinement method	Full-matrix least-squares on F^2	Full-matrix least-squares on F^2
Data/restraints/parameters	1601/0/120	2010/0/135
Goodness-of-fit on F^2	1.062	1.060
Final R indices [$I > 2\sigma(I)$]	0.025	0.033
R indices (all data)	0.031	0.038
Largest diff. peak and hole (e Å^{-3})	0.280, −0.440	0.620, −0.380

present compounds have only two of the squarato oxygens coordinating directly to the Ni(II) ion, forming a chain structure (figures 1 and 3).

In **1**, Ni(II) is *trans* connected to two molecules of 4-methylimidazole [Ni1–N1 = 2.068(2) Å] occupying the axial sites, two aqua ligands [Ni1–O1W = 2.095(2) Å] and two squarate-oxygen atoms [Ni1–O2 = 2.083(2) Å] composing the basal plane, adopting a slightly distorted octahedral geometry (figure 1). In **1**, the Ni1–$O_{squarate}$ bond distance is slightly shorter than the Ni–O_{aqua} bond because of the electronegative character of the $C_4O_4^{2-}$ ligand. The Ni–O_{aqua} bond lengths compare well with those observed in $[Ni(C_4O_4)(H_2O)_2]$ [2.060(9) Å] [32], $[Ni(C_4O_4)(Him)_2(H_2O)_2]$ [2.069(9) Å] [33], $[Ni(C_4O_4)(bipy)_2(H_2O)_2] \cdot 2H_2O$ [2.030(3) and 2.054(3) Å] (bipy: 2,2′-dipyridl) [34] and $[Ni(C_4O_4)(py)_2(H_2O)_2]$ [2.090(4) Å] (py: pyridine) [35], whereas the Ni–$O_{squarate}$ bond lengths are considerably shorter than those observed in the corresponding compounds. In **1**, the Ni1–N1 bond length is within the range of values reported for Ni–N distances [36, 37]. Angles for coordinated atoms to Ni(II) are near 90 or 180° without notable exception (table 2).

In **2**, each Ni(II) is hexa-coordinated by four nitrogens of two potentially bidentate symmetry related histamine ligands [Ni1–N1 = 2.085(2) Å and Ni1–N3 = 2.092(2) Å] and *cis*-coordinated two squarate-oxygens [Ni1–O1 = 2.154(1) Å], adopting a slightly distorted octahedral geometry (figure 3). In the crystal structure of **2**, there is also one water molecule. The Ni–$O_{squarate}$ bond distances in **2** are significantly longer than in **1**. Presumably, the strongly coordinated histamine ligands are responsible for the larger

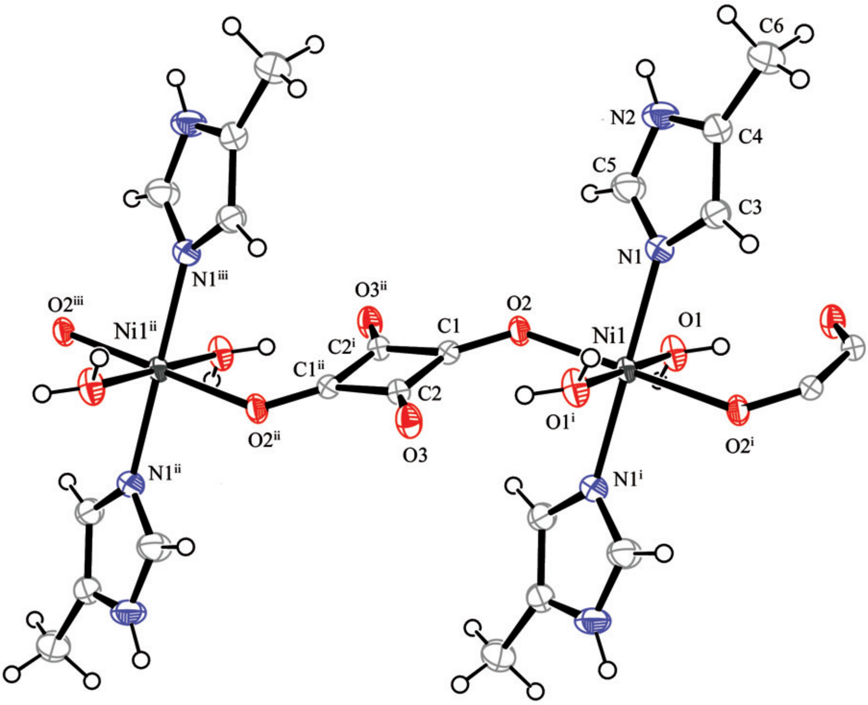

Figure 1. The molecular structure of **1** showing the atom-numbering scheme. Displacement ellipsoids are drawn at the 30% probability level and H atoms are shown as small spheres of arbitrary radii [symmetry codes (i): $-x$, $1-y$, $1-z$; (ii): $-x$, $2-y$, $1-z$; (iii): x, $1+y$, z].

Ni–O$_{\text{squarate}}$ distance. This lengthening of Ni–O$_{\text{squarate}}$ bond distances is also observed in other Ni(II)-squarate complexes having strong nitrogen donors [33–35]. In **2**, the best equatorial plane around the Ni(II) ion is comprised of O1, O1*, N3 and N3* atoms (symmetry code *: $1-x$, y, $1.5-z$), with the r.m.s. deviations of 0.050 Å and the largest deviation from the mean plane is 0.052 Å for atom O1; symmetry related N1 atoms are in the apical positions.

The squarate anions are almost planar in both compounds as expected. In **1**, the C–O [1.246(2) Å] bonds involving coordinated oxygens are slightly shorter than the other C–O [1.256(2) Å] bonds, while in **2** the C–O [1.257(2) Å] bonds involving coordinated oxygen are slightly longer than the other C–O [1.241(2) Å] bonds. The C–C bond lengths [1.460(2) and 1.464(2) Å for **1**, 1.462(3) and 1.468(2) Å for **2**] are slightly larger than the mean value in squaric acid [1.456(12) Å] and close to the value reported for $[Ni(C_4O_4)(Him)_2(H_2O)_2]$ [1.463(2) Å], $[Ni_2(tren)_2(H_2O)_2][ClO_4]_2$ [tren = *tris*(2-aminoethyl)amine] [1.469(3) Å] [38], but somewhat smaller than the value reported for $[Ni(C_4O_4)(H_2O)_2]$ [1.478(16) Å]. The O–C–C angles vary in the range 137.9(2)–132.4(2)° for **1** and 137.1(2)–132.5(2)° for **2**, whereas the C–C–C angles are very close to 90° in both compounds.

The imidazole ring is planar in both polymeric compounds, with r.m.s. deviations of 0.002 Å for **1** and 0.012 Å for **2**, with maximum deviations from this plane of 0.003 Å for atom C3 in **1** and 0.017 Å for atom C3 in **2**. These planes are approximately perpendicular to the squarate planes in both compounds, with a dihedral angle of 62.40(10)° for **1** and 73.25(10)° for **2**.

The crystal packing of both compounds, shown in figures 2 and 4, is formed via intra- and intermolecular hydrogen bonding interactions. In **1**, the chains are held together by strong hydrogen bridges between aqua ligands and the non-coordinated squarate oxygens, forming a two-dimensional array of Ni(II) ions. These planes are held together by hydrogen bonds between the imidazole N and the non-coordinated squarate oxygens. In **2**, the NH_2 and NH groups, solvent water molecule and uncoordinated squarate oxygen atoms are involved in inter-chain hydrogen bonds (see table 3 for details). These interactions form a layered structure. The shortest interchain $\text{Ni(II)}\cdots\text{Ni(II)}^{a}$ distance [symmetry codes: (a) $-x-0.5$, $y+0.5$, $-z+0.5$ for **1** and (a) $-x+1$, $-y$, $-z+1$ for **2**] is 7.341(2) Å for **1** and 7.365(6) Å for **2**, whereas the intrachain equivalent is $\text{Ni(II)}\cdots\text{Ni(II)}^{\text{ii or **}}$ [symmetry codes: (ii) $-x$, $2-y$, $1-z$ for **1** and (**)$-x+1.5$, $-y+0.5$, $-z+1$ for **2**] of 7.935(5) Å for **1** and of 8.303(8) Å for **2**.

Table 2. Selected bond lengths and angles of **1** and **2**.

1					
Ni1–N1	2.068(2)	C1–O2	1.246(2)	N1–Ni1–O2	90.30(6)
Ni1–O2	2.083(2)	C1–C2^{ii}	1.460(2)	N1–Ni1–O1W	86.92(7)
Ni1–O1W	2.095(2)	C1–C2	1.464(2)	O2–Ni1–O1W	84.30(6)
C5–N1	1.309(2)	C2–O3	1.256(2)	C1–C2–C1^{ii}	90.33(13)
2					
Ni1–N1	2.085(2)	C6–O1	1.257(2)	N1–Ni1–O1	91.72(6)
Ni1–N3	2.092(2)	C6–C7	1.462(3)	N3–Ni1–O1	172.11(7)
Ni1–O1	2.154(1)	C6–C7^{iv}	1.468(2)	N1–Ni1–N3	90.95(7)
C4–N2	1.361(3)	C7–O2	1.241(2)	C7–C6–C7^{iv}	90.43(14)

Symmetry codes: (ii) $-x$, $2-y$, $1-z$; (iv) $-x+0.5$, $-y+0.5$, $2-z$.

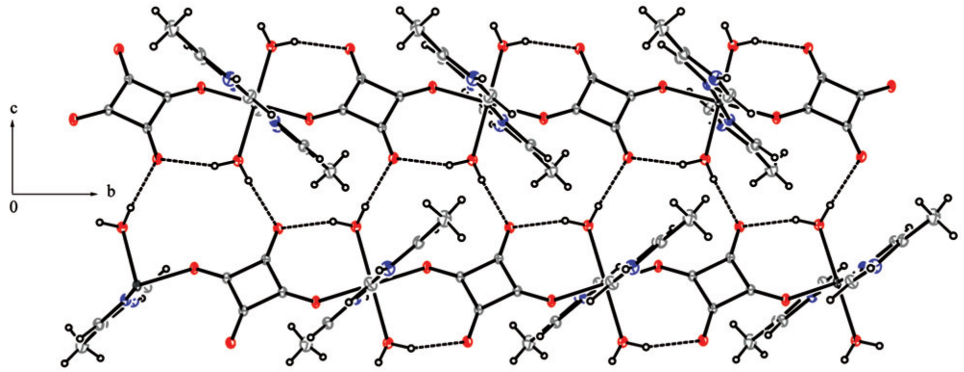

Figure 2. The chain structure of **1** along the crystallographic *b* axis, with intra- and interchain interactions indicated by dashed lines.

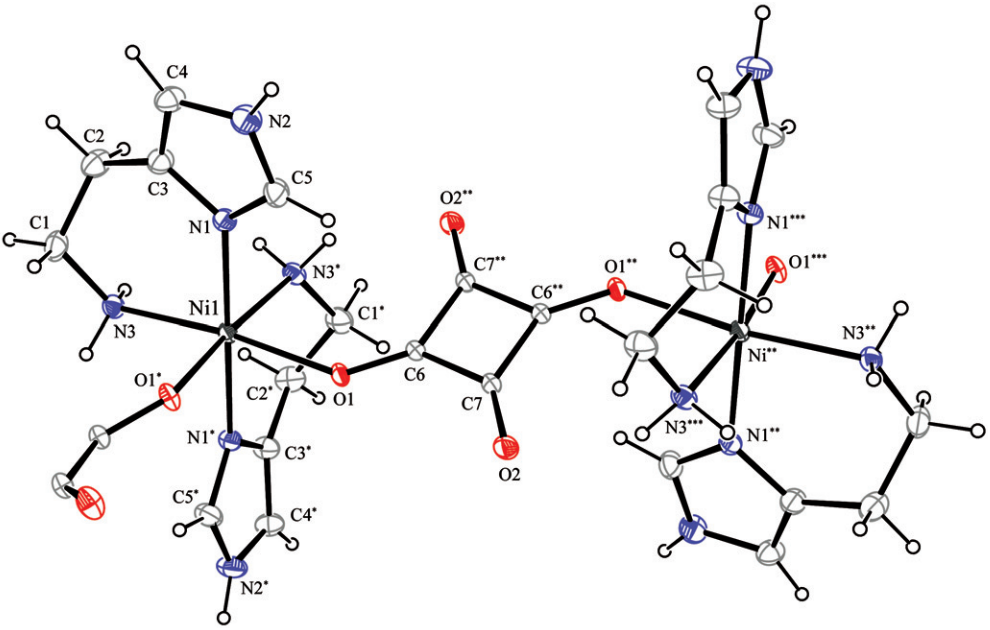

Figure 3. The molecular structure of **2** showing the atom-numbering scheme. Displacement ellipsoids are drawn at the 50% probability level and H atoms are shown as small spheres of arbitrary radii [symmetry codes; *: $1-x$, y, $1.5-z$; **: $1.5-x$, $0.5-y$, $1-z$; ***: $0.5+x$, $0.5-y$, $-0.5+z$].

3.2. *FT-IR investigation*

Infrared spectra of squarate-containing complexes are characteristic of the mode of coordination. Both compounds (figure 5) show broad and very intense bands at 1521 cm^{-1} (**1**), 1445 cm^{-1} and 1513 (**2**), assignable to a coupled mode of CO and CC stretching. The fact that this stretching vibration in both compounds is slightly split compared to the corresponding vibration in $K_2C_4O_4$ [39] strongly suggests the symmetry is lower than D_{4h}, confirmed by the X-ray investigation. Weak intensity IR

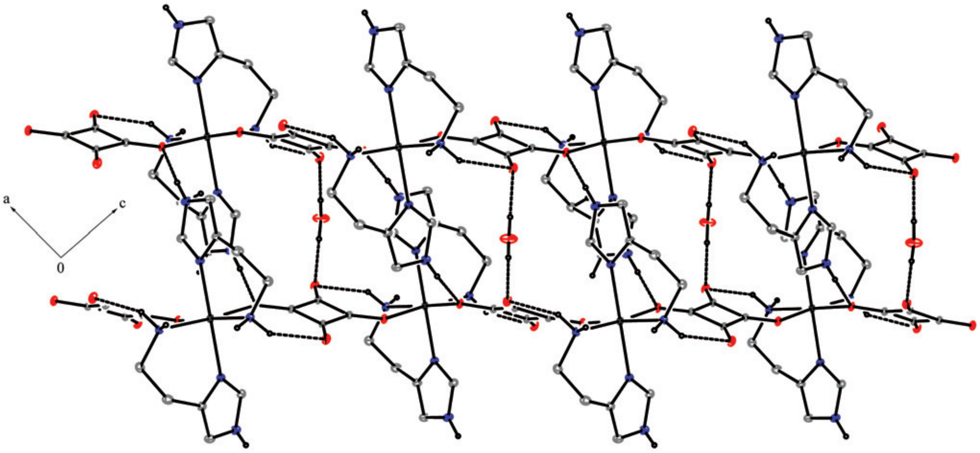

Figure 4. The chain structure of **2** with intra- and interchain interactions indicated by dashed lines.

Table 3. Hydrogen bonding interactions for **1** and **2** (Å, °).

	D–H···A	d(D–H)	d(H···A)	d(D···A)	∠(DHA)
Complex **1**	O1W–H1A···O3$^{\text{v}}$	0.84(3)	2.02(2)	2.850(3)	170(2)
	O1W–H1B···O3$^{\text{i}}$	0.81(3)	1.95(3)	2.722(2)	161(2)
	N2–H2···O3$^{\text{vi}}$	0.84(3)	2.08(3)	2.910(3)	168(3)
	OW1–H1···O2$^{\text{vii}}$	0.85(4)	1.90(4)	2.750(2)	176(4)
Complex **2**	N2–H2···O1$^{\text{viii}}$	0.95(4)	1.91(4)	2.828(3)	162(3)
	N3–H3A···O2***	0.74(3)	2.33(3)	2.982(2)	147(3)
	N3–H3A···OW1	0.87(3)	2.18(3)	3.012(3)	162(3)

Symmetry codes: (i) $-x, -y+1, -z+1$; (v) $x-0.5, -y+1.5, z-0.5$; (vi) $x+0.5, -y+1.5, z-0.5$; (vii) $x+0.5, y-0.5, z$; (viii) $x+0.5, -y+0.5, z+0.5$; (***) $x+0.5, -y+0.5, z-0.5$.

bands observed above 1550 cm^{-1} were taken as evidence for the presence of localized squarate C=O [1731 cm^{-1} for **1** and 1735 cm^{-1} for **2**] and C=C [1631 cm^{-1} for **1** and 1643 cm^{-1} for **2**]. These stretching vibrations were found at 1777 cm^{-1} and 1640 cm^{-1} in the IR spectra of free squaric acid. The weak absorption bands at 1594 cm^{-1} for **1** and 1577 cm^{-1} for **2** can be attributed to H–O–H bending of water. A strong and broad feature in the region 3500–3000 cm^{-1} in the IR spectra of both compounds is indicative of the presence of N–H···O and O–H···O hydrogen bonds. The OH/NH frequency range implies that neither the water molecules nor the imidazole NH groups participate in very strong hydrogen bonds. Moreover, the existence of ν(OH) bands close to 3500 cm^{-1} indicate that some of the water OH groups are very weakly hydrogen bonded. Considering the chemical structure of histamine, the vibration band information on metal coordination of histamine mainly originates from the symmetric and asymmetric stretching vibrations of NH_2. The vibration of the NH_2 at 3272–3100 cm^{-1} is higher than free histamine. This shift clearly indicates that histamine coordinates to nickel(II) through NH_2. The 936 cm^{-1} ring mode of free imidazole [40] is strongly dependent on the coordination geometry of the complexes. In **1**, this band is displaced to higher energies after coordination (946 cm^{-1}) and its intensity is strongly enhanced. Most of the other skeletal vibrations are unaffected by coordination.

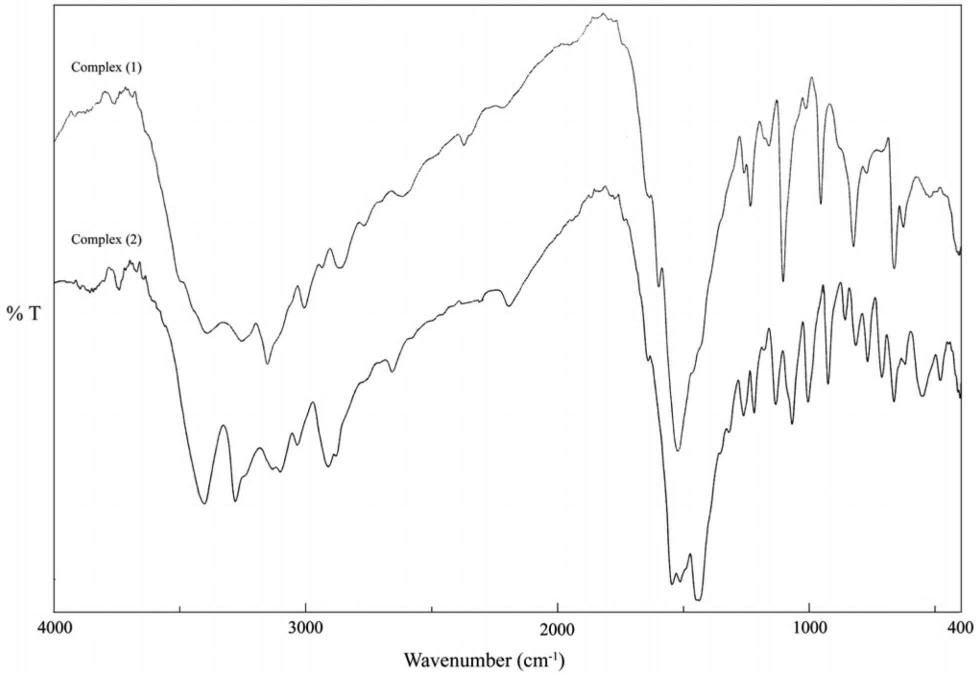

Figure 5. The FT-IR spectra of **1** and **2**.

3.3. *UV-Vis spectra*

The UV spectra of both complexes display a band centered at 275 nm (**1**) and 282 nm (**2**) corresponding to absorption within the squarate anion. The position of this band is insensitive to the mode of coordination [41]. In addition, in the UV region both spectra display a broad band at 210 nm (**1**) and 217 nm (**2**), due to $\pi \rightarrow \pi^*$ intraligand transitions of the 4-*Meim* and *his* ligands, respectively. The visible spectra of both compounds are very similar. The d–d transition spectrum in aqueous solution is compatible with a distorted octahedral configuration. The λ_{max} values at 545 and 890 nm for **1** and 574 and 900 nm for **2** were assigned to ν_2: $^3A_{2g} \rightarrow {}^3T_{1g}$ and ν_1: $^3A_{2g} \rightarrow {}^3T_{2g}$ d–d transitions.

3.4. *Voltammetric behavior of 1 and 2*

The redox behavior of $C_4H_2O_4$ (squaric acid) in acidic media have been reported in the literature [42]. Squarate anion and its monosubstituted derivatives can be oxidized reversibly in two consecutive steps to the corresponding radical monoanions and neutral forms [$E_{1/2} = -0.120$ V and $E_{1/2} = 0.810$ V *versus* SCE (Saturated Calomel Electrode) for $C_4O_4^{2-}$] [43].

The cyclic voltammograms of **1** and **2** in 5 mM solution at a platinum wire electrode with **DMF** (dimethylformamide) as the solvent are shown in figure 6. No evidence of Ni(II) oxidation or reduction in the potential range from −0.20 to 1.40 V is observed in the compounds (figure 6a). Compound **1** yields oxidation peaks at 0.38 and 0.84 V in the anodic branch, and two reduction peaks at 0.30 and 0.68 V on the

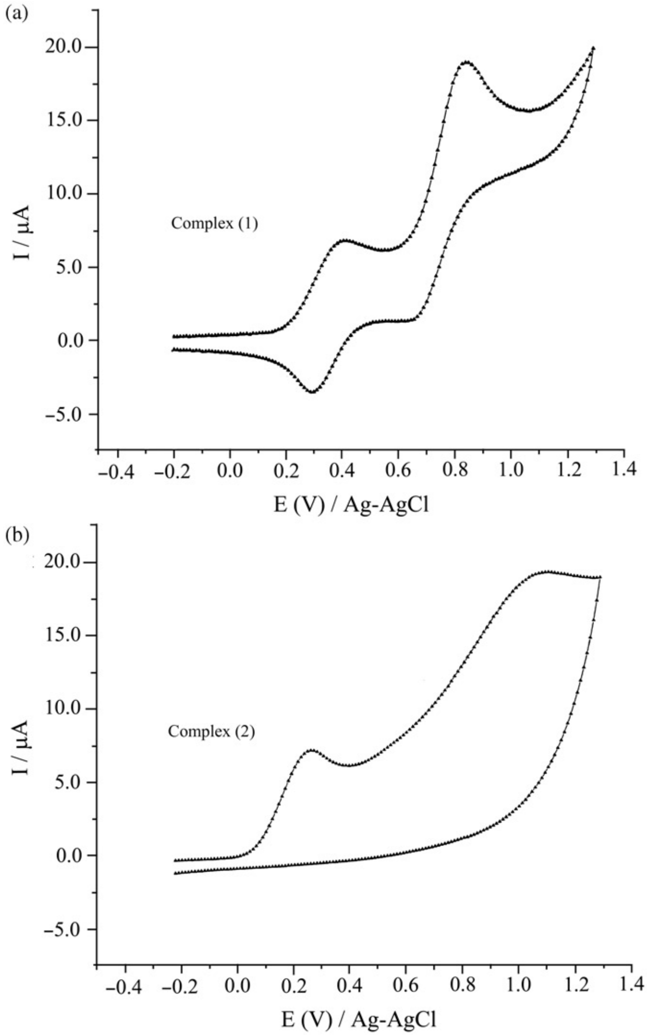

Figure 6. The cyclic voltammograms of (**1**) **(a)** and (**2**) **(b)** in a solution of 5 mM complexes at a Pt wire electrode in 0.1 M DMSO- n-Bu_4NClO_4, potential scan rate 100 mVs^{-1} (potential scanning starts at −0.2 V towards anodic potential and back to 0.0 V and towards negative potential).

reverse scan (figure 6a). As already mentioned, these redox couples correspond to two successive monoelectronic oxidations and reductions of $C_4O_4^{2-}$. The first step is oxidation of the dianion into the radical anion,

$$\mathrm{Sq}^{2-} \Leftrightarrow \mathrm{Sq}^{-\bullet} + e^{-}\left(E_{1/2} = 0.34\,\mathrm{V}\ vs.\ \frac{\mathrm{Ag}}{\mathrm{AgCl}}\right)$$

and the second corresponds to oxidation of the radical anion into the neutral form,

$$\mathrm{Sq}^{-\bullet} \Leftrightarrow \mathrm{Sq} + e^{-}\left(E_{1/2} = 0.76\,\mathrm{V}\ vs.\ \frac{\mathrm{Ag}}{\mathrm{AgCl}}\right).$$

The second electron transfer induces loss of π delocalization as in electrooxidation of the squarate dianion Sq^{2-} into the instable tetraacetone C_4O_4. As can be seen in figure 6a, the ratio of peak current (I_{pc}/I_{pa}) is 0.8 for $E_{1/2}$ and 0.5 for $E_{1/2}$. However, the peak current increases with increase of the square root of the scan rate ($50\,mVs^{-1} - 500\,mVs^{-1}$). The $I_p/v^{1/2}$ value is almost constant for all scan rates, establishing the electrode process as diffusion controlled. ΔEp ($=E_{pa} - E_{pc}$) provides a rough evaluation of the degree of reversibility of electron transfer. ΔEp of the peaks is greater than $59/n$ mV, where n is the number of the electrons transferred, and increases with increasing scan rate. Therefore, the electron transfer process is not in equilibrium and shown to be slow. From all the voltammetric data, the redox couples of **1** can be attributed to the electrode reaction of the dianion Sq^{2-} within a quasi-reversible 1e-transfer process.

In **2**, the squarate anion yields only two irreversible oxidation peaks at 0.28 and 1.02 V in the anodic branch (figure 6b).

4. Conclusions

Two new squarate complexes of nickel(II), $[Ni(C_4O_4)(4\text{-Meim})_2(H_2O)_2]_n$ (**1**) and $[Ni(C_4O_4)(his)_2]_n \cdot nH_2O$ (**2**), have been synthesized. Structural study indicates both compounds have distorted octahedral geometry with infinite chain structures. The OH/NH vibration bands in both compounds imply that neither the water molecule nor the imidazole NH groups participate in strong hydrogen bonds. The observed d–d transitions in the UV-Vis spectra of both compounds are compatible with a distorted octahedral configuration. Both the IR and the UV-Vis results are consistent with the structural data. The electrochemical data showed that both compounds have two consecutive oxidation steps in the cyclic voltammogram similar to the electrochemical behavior of squarate ligand implying the free form of the ligand in aqueous solution.

Supplementary data

Crystallographic data (excluding structure factors) for the structure in this paper have been deposited with the Cambridge Crystallographic Data Centre as the supplementary publication no. CCDC 636091 for **1** and CCDC 636092 for **2**. Copies of the data can be obtained, free of charge, on application to CCDC, 12 Union Road, Cambridge, CB12 1EZ, UK (Fax: +44 1223 366 033; Email: deposit@ccdc.ac.uk or on the www: http://www.ccdc.cam.ac.uk).

Acknowledgement

I would like to thank Prof Dr Orhan Büyükgüngör for the acquisition of XRD data.

References

[1] G. Seitz, P. Imming. *Chem. Rev.*, **92**, 1227 (1992).
[2] L.S. Liebeskind, M.S. Yu, R.H. Yu, J. Wang, K.S. Hager. *J. Am. Chem. Soc.*, **115**, 9048 (1993).
[3] J.T. Reinprecht, J.G. Miller, G.C. Vogel, M.S. Haddad, D.N. Hendrickson. *Inorg. Chem.*, **19**, 927 (1980).
[4] J.A.C. van Ooijen, J. Reedijk, A.L. Spek. *Inorg. Chem.*, **18**, 1184 (1978).
[5] D.S. Yufit, D.J. Price, J.A.K. Howard, S.O.H. Gutchke, A.K. Powal, P.T. Wood. *Chem. Commun.*, 1561 (1999).
[6] J.C. Trombe, L. Sabadie, P. Milet. *Solid State Sci.*, **4**, 1209 (2002).
[7] P. Milet, L. Sabadie, J. Galy, J.C. Trombe. *J. Solid State Chem.*, **173**, 49 (2003).
[8] G. Bernardinelli, D. Deguenon, R. Soules, P. Castan. *Can. J. Chem.*, **67**, 1185 (1989).
[9] R.R. Lee, C.C. Wang, Y. Wang. *Acta Cryst.*, **B52**, 966 (1996).
[10] M. Beneto, L. Soto, J.G. Lozano, E. Escriva, J.P. Legros, F. Dahan. *J. Chem. Soc., Dalton Trans.*, 1057 (1991).
[11] İ. Uçar, A. Bulut, O. Büyükgüngör, A. Karadağ. *Trans. Met. Chem.*, **31**, 1057 (2006).
[12] C.H. Yang, C.H. Chuo, G.H. Lee, C.C. Wang. *Inorg. Chem. Commun.*, **6**, 135 (2003).
[13] X. Solans, M. Agiuilo, A. Gleizes, J. Faus, M. Julve, M. Verdauger. *Inorg. Chem.*, **29**, 775 (1990).
[14] I. Castro, M.L. Calatayud, J. Sletten, F. Lloret, M. Julve. *J. Chem. Soc., Dalton Trans.*, 811 (1997).
[15] A. Crispini, D. Pucci, I. Aiello, M. Ghedini. *Inorg. Chim. Acta*, **304**, 219 (2002).
[16] I. Castro, J. Sletten, M.L. Calatayud, M. Julve, M. Cano, F. Lloret, A. Caneshi. *Inorg. Chem.*, **34**, 4903 (1995).
[17] L. Lisnard, P. Mialane, A. Dolbecq, J. Marrot, F. Secheresse. *Inorg. Chem. Commun.*, **6**, 503 (2003).
[18] B. Modec, J.V. Brencic, E.M. Burkholder, J. Zubieta. *Dalton Trans.*, 4618 (2003).
[19] P.M. Piggot, L.A. Hall, A.J. White, D.J. Williams. *Inorg. Chim. Acta*, **1**, 207 (2004).
[20] A. Bulut, İ. Uçar, O.Z. YeŞilel, H. İçbudak, H. Ölmez, O. Büyükgüngör. *Acta Cryst.*, **C60**, m526 (2004).
[21] İ. Uçar, A. Bulut, O. Büyükgüngör. *Acta Cryst.*, **C61**, m266 (2005).
[22] İ. Uçar, A. Bulut. *Acta Cryst.*, **E61**, m2730 (2005).
[23] İ. Uçar, H. PaŞaoğlu, O. Büyükgüngör, A. Bulut. *Acta Cryst.*, **E61**, 1405 (2005).
[24] İ. Uçar, A. Bulut. *Acta Cryst.*, **E61**, 1320 (2005).
[25] İ. Uçar, A. Bulut, O. Büyükgüngör. *Acta Cryst.*, **C61**, m218 (2005).
[26] İ. Uçar, A. Bulut, C. Kazak. *Acta Cryst.*, **C61**, m428 (2005).
[27] H. Tamura, H. Imai, J. Kuwahara, Y. Sugiura. *J. Am. Chem. Soc.*, **109**, 6870 (1987).
[28] A.C. Andrews, T.D. Lyons, T.D. O'Brien. *J. Chem. Soc.*, **84**, 1776 (1962).
[29] Stoe & Cie. *X-AREA (Version 1.18) and X-RED (Version 1.04)*, Stoe & Cie, Darmstadt, Germany (2002).
[30] G.M. Sheldrick. *SHELXL97, A program for Crystal Structure Refinement*, University of Göttingen, Germany (1997).
[31] M.N. Burnett, C.K. Johnson. *ORTEPIII*. Report ORNL-6895, Oak Ridge National Laboratory, Tennessee, U.S.A (1996).
[32] M. Habenschuss, B.C. Gerstein. *J. Chem. Phys.*, **62**, 852 (1974).
[33] J.A.C. Ooijen, J. Reedijk, A.L. Spek. *Inorg. Chem.*, **18**, 1184 (1979).
[34] R. Soules, F. Dahan, J.P. Laurent, P. Castan. *J. Chem. Soc., Dalton Trans.*, 587 (1988).
[35] R. Kirchmaier, E. Altin, A. Lentz. *Z. Kristallogr.*, **218**, 1 (2003).
[36] İ. Uçar, A. Bulut. *Acta Cryst.*, **E61**, m2730 (2005).
[37] O.Z. Yesilel, A. Bulut, I. Uçar, H. İçbudak, H. Ölmez, O. Büyükgüngör. *Acta Cryst.*, **E60**, m228 (2004).
[38] I. Castro, M.L. Calatayud, J. Sletten, F. Lloret, M. Julve. *J. Chem. Soc., Dalton Trans.*, 811 (1997).
[39] M. Ito, B. West. *J. Am. Chem. Soc.*, **85**, 2580 (1963).
[40] W.J. Davis, J. Smith. *J. Chem. Soc. A*, 317 (1971).
[41] J.T. Reintprecht, J.G. Miller, G.C. Vogel, M.S. Haddad, D.N. Hendrickson. *Inorg. Chem.*, **19**, 927 (1980).
[42] A. Rodes, J.M. Orts, J.M. Perez, J.M. Feliu, A. Aldaz. *J. Electroanal. Chem.*, **421**, 195 (1997).
[43] G. Farnia, G. Sandona. *J. Electroanal. Chem.*, **348**, 339 (1993).